16th ICAAR
LISBOA 2020-2022

16th International Conference on
Alkali-Aggregate Reaction in Concrete
Lisboa | LNEC | Portugal | 31 May - 2 June 2022

http://icaar2020-2022.lnec.pt

Solubility data for alkali-silica reaction products

Barbara Lothenbach (1), (2), Zhenguo Shi (1)

(1) Laboratory for Concrete & Construction Chemistry, Swiss Federal Laboratories for Materials Science and Technology (Empa), 8600 Dübendorf, Switzerland, barbara.lothenbach@empa.ch, zhenguo.shi@empa.ch

(2) Department of Structural Engineering, Norwegian University of Science and Technology (NTNU), 7491 Trondheim, Norway

Abstract

Alkali-silica reaction (ASR) can cause expansion and cracking of concrete. The reaction products formed within the aggregates are difficult to characterize due to the micro-scale volume of the reaction products. Although ASR has been extensively investigated over the past decades, many aspects are still unclear, such as the thermodynamic stability of ASR products. Thus, predictions of the occurrence of ASR and the resulting expansion of concrete are difficult. In this study, the solubility of different synthetic ASR products is determined at different temperatures (i.e., 20, 40, 60 and 80 °C), based on the experimental solubility data collected from dissolution of ASR products, synthesized at 80 °C, i.e., K-shlykovite, Na-shlykovite and ASR-P1. The solubility products of K-shlykovite, Na-shlykovite and ASR-P1 show a moderate destabilisation with increasing temperature. Application of these solubility products indicated that low Ca/Si and intermediate alkali concentration favour the formation of ASR products, while a higher availability of Ca and/or very high alkali concentrations suppress the formation of ASR products.

***Keywords**: alkali-silica reaction; shlykovite; ASR-P1; C-S-H; solubility*

1. INTRODUCTION

Alkali-silica reaction (ASR) occurs due to the interaction between reactive silica in concrete aggregates and alkali hydroxide from the pore solution of the cement. This reaction can result in expansion and cracking of the concrete, and thus significantly shorten the service life of concrete infrastructure. Although ASR has been studied over 80 years since it was first reported in 1940 [1], the knowledge about the factors controlling and limiting ASR is insufficient. The main challenge to understand ASR and the resulting damage is associated with the difficulties to characterize the ASR products formed in concrete aggregates, as the size of these reaction products is very small [2]. The lack of knowledge, in particular of the solubility of ASR products, makes the prediction of the occurrence of ASR impossible. The availability of experimental solubility data, would allow to use thermodynamic modelling to understand better under which conditions ASR products are less probable to form.

Thermodynamic models have been developed to describe the solubility of C-S-H depending on Ca/Si, Al/Si and pH [3,4] and used to predict the composition of hydrated cement. Unfortunately, no thermodynamic models based on measured solubility data are available for ASR products. First attempts of applying thermodynamic models to ASR have been made [5,6]. Kim and Olek [5] used estimated solubilities for two hypothetical ASR products ($K_2Ca_4Si_6O_{17}\cdot10.5H_2O$ and $Na_2Ca_4Si_6O_{17}\cdot10.5H_2O$) to describe the sequence of ASR. Guthrie and Carey [6] used magadiite ($NaSi_7O_{14}\cdot4.5H_2O$) as a crystalline surrogate for an alkali-silicate and okenite ($CaSi_2O_5\cdot2H_2O$) as a surrogate for a high calcium-silicate ASR product. These calculations showed that it is in principle possible to predict the limiting conditions for formation of ASR products and highlight the need to determine their solubility products.

Recently, crystalline ASR products (K-shlykovite: $KCaSi_4O_8(OH)_3\cdot2H_2O$; Na-shlykovite: $NaCaSi_4O_8(OH)_3\cdot2.3H_2O$) and nanocrystalline (ASR-P1: $K_{0.52}Ca_{1.16}Si_4O_8(OH)_{2.84}\cdot1.5H_2O$) ASR products have been synthesized at 80°C [7]. It was observed that both K- and Na-shlykovite had strong similarity in chemical composition and molecular structure to the ASR products formed in concrete, which has a layered silicate structure with its SiO_4^{4-} tetrahedron charge balanced by K^+ and Ca^{2+} in the main layer and by H^+ in the interlayer. In particular Raman spectra showed that K-shlykovite was structurally identical to the ASR products formed in concrete aggregates during concrete prism test at 60 °C [7]. A silicate sheet structure was also observed for the nanocrystalline ASR-P1, which is stabilised at slightly higher Ca concentrations than K-shlykovite [7]. The observed strong similarity between the synthesized

ASR products and those in concrete aggregates supports the use of such synthesized ASR products for further understanding ASR and to measure the solubility of ASR products.

Different ASR products were synthesized to experimentally determine the solubility of K-shlykovite, Na-shlykovite and ASR-P1 at 20, 40, 60 and 80°C and to investigate the effect of the initial Ca/Si ratio and alkali/Si ratio on the stable ASR products using thermodynamic modelling.

2. MATERIALS AND METHODS

2.1 Dissolution experiments

K-shlykovite, ASR-P1 and Na-shlykovite were synthesised at 80°C from amorphous SiO_2 (hydrophilic silica, surface area 200 m^2/g, from EVONIK industries), CaO (obtained by burning calcium carbonate for 12 h at 1000 °C) and analytical KOH (≥ 85% KOH basis) or NaOH (≥ 99.9% NaOH basis) pellets as detailed in [7]. In addition to K-shlykovite, ASR-P1 and Na-shlykovite, minor amounts of C-S-H were also present in the samples before dissolution [7]. In order to determine the solubility, 0.6 g of either K-shlykovite, ASR-P1 or Na-shlykovite was dissolved in 10 g of MilliQ water at 20, 40, 60 and 80 °C for one month. Afterwards, the pH and chemical compositions of the filtrate were measured with a Knick pH meter and by ion chromatography (IC), while the solid phases present after the reaction were determined by Raman spectroscopy.

2.2 Methods

Thermodynamic modelling was performed using the Gibbs free energy minimization software GEMS v3.3 [8,9]. GEMS can be used to calculate the thermodynamic equilibrium and predict the compositions in a system composed of aqueous, solid and gaseous phases at the temperature and pressure of interest by minimizing the Gibbs free energy of the system. The calculations were carried out using the PSI/Nagra general thermodynamic database [10] and the Cemdata18 database [11] to calculate the elemental concentration in solution and the solid phases expected to precipitate at 80 °C. The solubility data were completed with those for the model ASR products Na-shlykovite, K-shlykovite and ASR-P1, obtained experimentally in this study. For C-S-H, the CNASH model developed by Myers et al. [12] was used, completed with an additional K-endmember with a stability 0.5 log units lower than the one of the Na-endmember as detailed in [13].

Based on the chemical composition of the solid and the measured aqueous concentrations, the solubility products were calculated:

$$\text{K-shlykovite: } \mathrm{K_{S0}(KCaSi_4O_8(OH)_3 \cdot 2H_2O)} = \frac{\mathrm{\{K^+\}\cdot\{Ca^{2+}\}\cdot\{SiO_2^0\}^4\cdot\{OH^-\}^3\cdot\{H_2O\}^2}}{\mathrm{\{KCaSi_4O_8(OH)_3\cdot 2H_2O\}}} \tag{1}$$

$$\text{ASR-P1: } \mathrm{K}_{S0}(K_{0.52}Ca_{1.16}Si_4O_8(OH)_{2.84} \cdot 1.5H_2O) = \frac{\{K^+\}^{0.52}\cdot\{Ca^{2+}\}^{1.16}\cdot\{SiO_2^0\}^4\cdot\{OH^-\}^{2.84}\cdot\{H_2O\}^{1.5}}{\{\mathrm{K}_{0.52}Ca_{1.16}Si_4O_8(OH)_{2.84}\cdot 1.5H_2O\}} \tag{2}$$

$$\text{Na-shlykovite: } \mathrm{K_{S0}(NaCaSi_4O_8(OH)_3 \cdot 2.3H_2O)} = \frac{\mathrm{\{Na^+\}\cdot\{Ca^{2+}\}\cdot\{SiO_2^0\}^4\cdot\{OH^-\}^3\cdot\{H_2O\}^{2.3}}}{\mathrm{\{NaCaSi_4O_8(OH)_3\cdot 2.3H_2O\}}} \tag{3}$$

where {} denotes the activity of the species calculated by GEMS from the measured concentrations. The activity of a pure solid phase is equal to 1 by definition. The activity of a dissolved species, {i}, is related to its molal concentrations [c_i] (in mol/kg H_2O) by the dimensionless activity coefficient, γ: $\{c_i\} = \gamma_i[\mathrm{c}_i]$.

The effect of temperature on the solubility was expressed with the so-called 3-term approximation [16]:

$$\log K_T = A_0 + \frac{A_2}{T} + A_3 \ln T \tag{4}$$

$$\mathrm{A_0} = \frac{0.4343}{\mathrm{R}}\cdot\left[\Delta_r S^0_{T_0} - \Delta_r Cp^0_{T_0}(1+\ln T_0)\right],\ \mathrm{A_2} = \frac{0.4343}{\mathrm{R}}\cdot(\Delta_r H^0_{T_0} - \Delta_r Cp^0_{T_0}\, T_0),\ \mathrm{A_3} = \frac{0.4343}{\mathrm{R}}\cdot\Delta_r Cp^0_{T_0}$$. If

If the entropy ($S°$), the enthalpy ($\Delta_f H°$) and the heat capacity, $C°_p$, are known, the constants can be calculated directly; alternatively they can be fitted to the experimental solubility data [17].

3. RESULTS AND DISCUSSION

3.1 Solubility products for ASR products

The measured elemental concentrations of the aqueous solutions after one month of dissolution experiments are shown in Figure 3.1 for the different ASR products. The results show that all samples have very low calcium concentrations of below 1 mM. The silicon and alkali concentrations increase with temperature; the measured silicon concentrations are between 30 and 70 mM, while the total alkali concentrations are approximately 10 mM higher than the Si concentrations. In comparison with the chemical compositions of the solids, these observations indicate that some additional C-S-H precipitated during the dissolution of the ASR products. For ASR-P1, in addition to K also a significant amount of Na was measured in the solution, although only a negligible amount of Na was detected in the solids based on SEM/EDS analysis in a previous study [13]. It should be noted that a certain amount of Na was present during the synthesis of ASR-P1 [13], although Na was not incorporated into the solids. As the samples had not been washed, the Na present at the surface of the solids during drying has been transferred into these experiments.

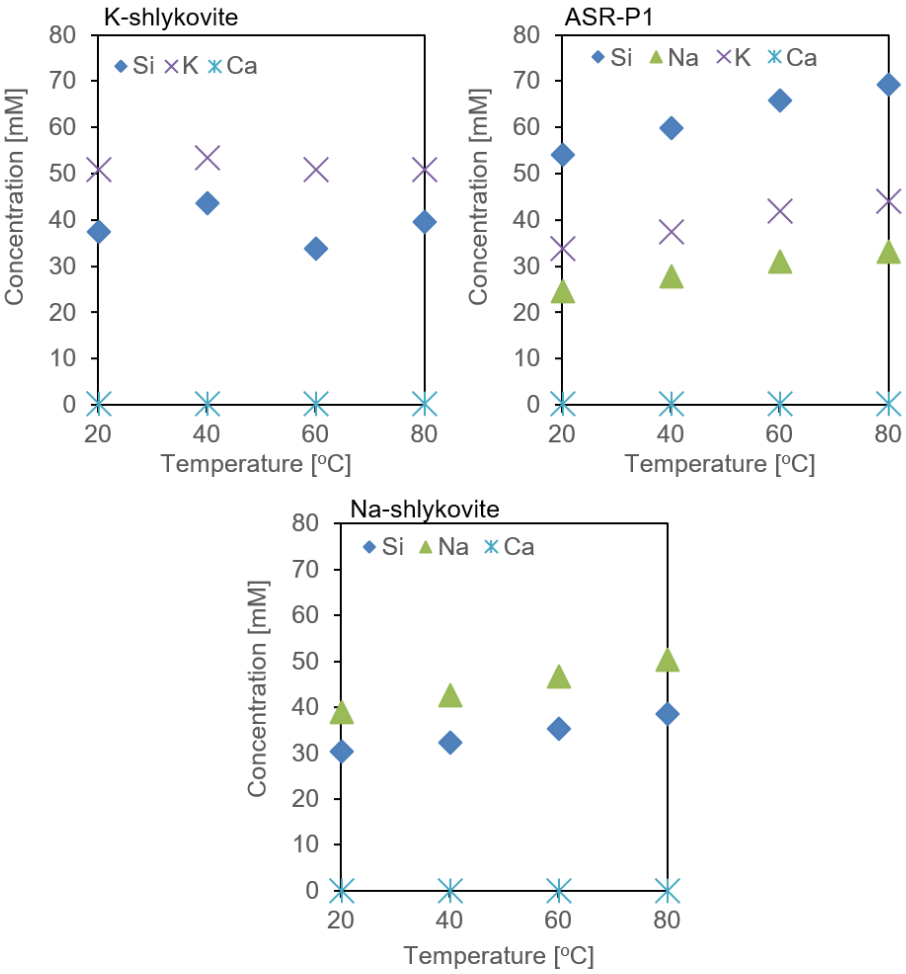

Figure 3.1: Measured elemental concentration of the samples after one month of dissolution.

Based on the measured concentrations in the dissolution experiments and the chemical compositions of the solids determined by SEM/EDS in [13], K-shlykovite: $KCaSi_4O_8(OH)_3 \cdot 2H_2O$; Na-shlykovite: $NaCaSi_4O_8(OH)_3 \cdot 2.3H_2O$ and nanocrystalline ASR-P1: $K_{0.52}Ca_{1.16}Si_4O_8(OH)_{2.84} \cdot 1.5H_2O$, the solubility products at 20, 40, 60 and 80°C were calculated using the thermodynamic software GEMS, as summarised in Figure 3.2. In all cases, the solubility increased slightly with temperature indicating a destabilisation of ASR-P1, Na- and K-shlykovite with increasing temperature. The observed increase of solubility was described by fitting the entropy S, while the heat capacity was estimated for the different ASR products according to equation (4). As shown in Figure 3.2, this is well able to describe the solubility of different ASR products as a function of temperature.

The results indicate that the ASR-P1, Na- and K-shlykovite, i.e. the high-temperature ASR products investigated in this study, are expected to be stable between 20 and 80°C, but that they become somewhat less stable at higher temperature. However, it should be noted that at 20 and 40°C different ASR products have been observed to precipitate than at 60°C and above, as recently reported in [14]. No low temperature ASR products have been observed to form during the dissolution experiments reported here, indicating a kinetic hindrance in the formation of the different solids at 40°C and below.

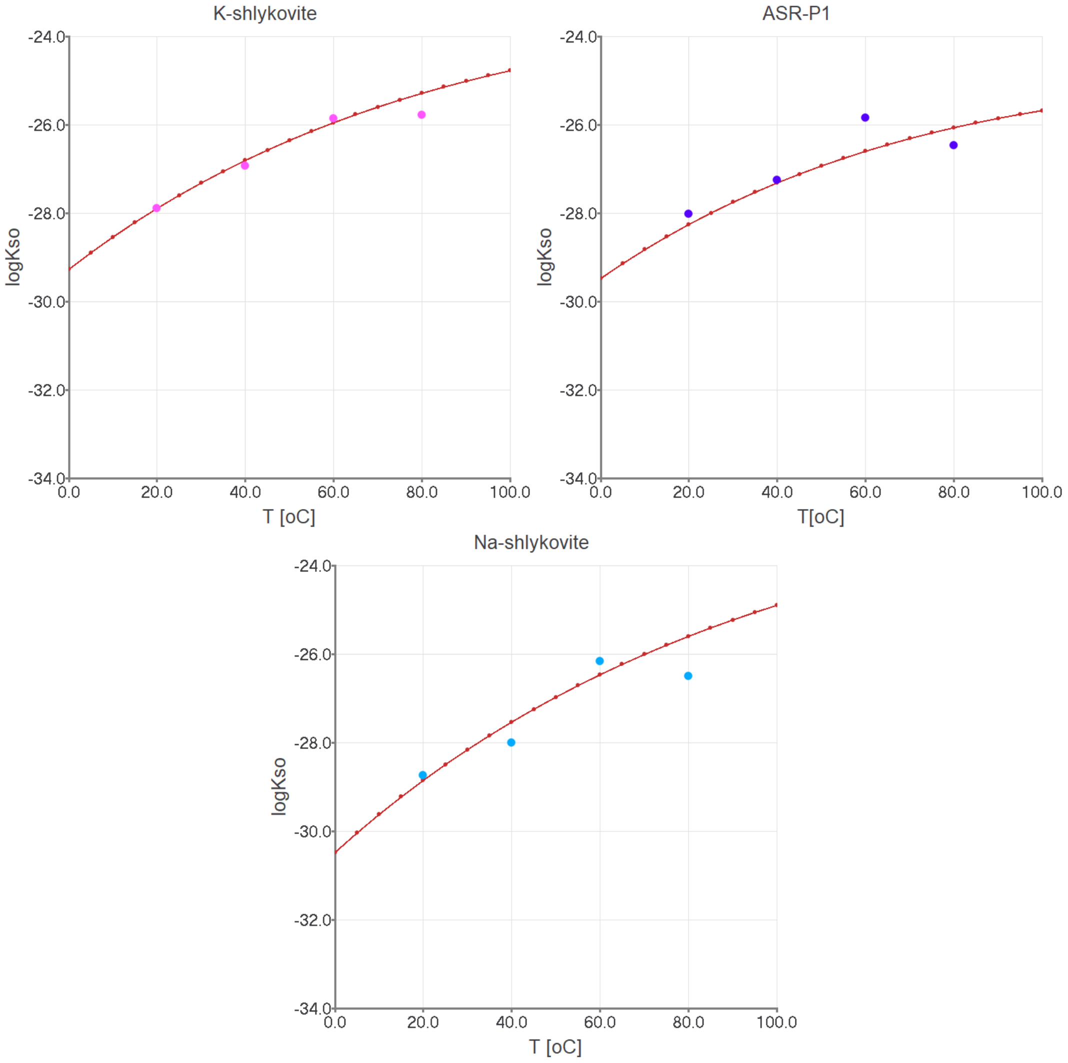

Figure 3.2: Solubility products for the K-shlykovite, ASR-P1 and Na-shlykovite calculated based on measured aqueous concentrations after dissolution experiments.

3.2 Calculation of the formation conditions of ASR products

Based on the derived thermodynamic data for K-shlykovite, ASR-P1 and Na-shlykovite at different temperatures, "favourable" formation conditions of ASR products can be predicted. Figure 3.3 shows the reaction sequences at either different initial Ca/Si or K/Si ratios at 60 °C. The results show that the amount of ASR products formed first increases and then decreases with increasing initial Ca/Si ratio, when the initial K/Si ratio is fixed at 0.5. This means that the presence of a certain amount of calcium is necessary to form ASR products. However, above Ca/Si = 0.2 some C-S-H is formed, while the amount of ASR products is reduced at higher Ca/Si, indicating that too much calcium can destabilize the ASR products to C-S-H.

Figure 3.3b) shows the effect of K at an initial Ca/Si ratio of 0.3. The amount of ASR products formed increases in the presence of more K but decreases at K/Si above 0.2. This suggests that although the presence of some K (or Na) to essential to form ASR products, too much alkalis can supress the formation of ASR products. This agrees well with the observation that very high alkali contents tend to reduce the ASR expansion in concrete samples [18] and in NaOH-activated slag mortars [19].

In both calculations, either at fixed initial K/Si ratio of 0.5 or at Ca/Si ratio = 0.3, a maximum amount of ASR products is predicted. Similar calculations had also been conducted for Na- and K-samples at 80 °C [13,15], which showed comparable results as those shown in Figure 3.3.

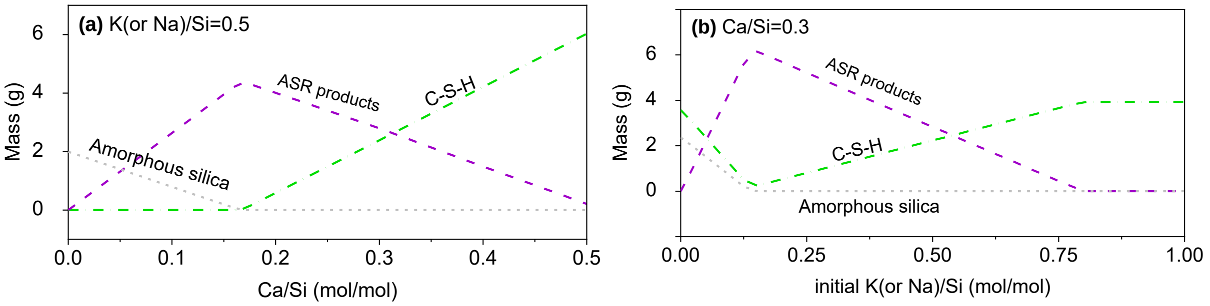

Figure 3.3: ASR sequence predicted at 60 °C. a) Effect of initial K/Si or Na/Si ratio on the formation of ASR products at a constant initial Ca/Si ratio of 0.3. b) Effect of Ca/Si ratio on formation of ASR products at a constant initial K/Si ratio of 0.5.

4. CONCLUSIONS

In this study, the solubility products of the ASR products synthesized at 80°C (i.e. K-shlykovite, ASR-P1 and Na-shlykovite) have been measured between 20 and 80°C. Based on these solubility products, the "favourable" formation conditions of ASR products were calculated to be at Ca/Si of ≈0.2 and K/Si ≈0.2. A higher availability of both K and/or Ca leads to the stabilisation of C-S-H instead of ASR products. The results confirm also that ASR products can coexist with C-S-H and that the formation of the different ASR products depends on the availability of Ca and alkali ions.

It is expected that the further development of thermodynamic data for ASR products (not only for the ASR products formed at high temperature, but also for those ASR products observed at 40 ° and below), will contribute to better understand of the formation conditions of ASR products in concrete.

5. ACKNOWLEDGEMENTS

The authors would like to acknowledge the financial support of Z. Shi by SNF Sinergia: Alkali-silica reaction in concrete (ASR), grant number CRSII5_17108 and the European Union's Horizon 2020 research and innovation programme under the Marie Skłodowska-Curie grant agreement number 754364.

6. REFERENCES

[1] T.E. Stanton, Influence of cement and aggregate on concrete expansion, Eng. News-Record. 1 (1940) 59–61.

[2] A. Leemann, T. Katayama, I. Fernandes, M.A.T.M. Broekmans, Types of alkali–aggregate reactions and the products formed, Proc. Inst. Civ. Eng. Mater. 169 (2016) 128–135. https://doi.org/10.1680/jcoma.15.00059.

[3] D.A. Kulik, Improving the structural consistency of CSH solid solution thermodynamic models, Cem. Concr. Res. 41 (2011) 477–495. https://doi.org/10.1016/j.cemconres.2011.01.012.

[4] R.J. Myers, J.L. Provis, B. Lothenbach, Composition–solubility–structure relationships in calcium (alkali) aluminosilicate hydrate (C-(N, K-) ASH), Dalt. Trans. 44 (2015) 13530–13544. https://doi.org/10.1039/C5DT01124H.

[5] T. Kim, J. Olek, Chemical Sequence and Kinetics of Alkali–Silica Reaction Part II. A Thermodynamic Model, J. Am. Ceram. Soc. 97 (2014) 2204–2212. https://doi.org/10.1111/jace.12830.

[6] G.D. Guthrie, J.W. Carey, A thermodynamic and kinetic model for paste–aggregate interactions and the alkali–silica reaction, Cem. Concr. Res. 76 (2015) 107–120. https://doi.org/10.1016/j.cemconres.2015.05.004.

[7] Z. Shi, G. Geng, A. Leemann, B. Lothenbach, Synthesis, characterization, and water uptake property of alkali-silica reaction products, Cem. Concr. Res. 121 (2019) 58–71. https://doi.org/10.1016/j.cemconres.2019.04.009.

[8] D.A. Kulik, T. Wagner, S. V Dmytrieva, G. Kosakowski, F.F. Hingerl, K. V Chudnenko, U.R. Berner, GEM-Selektor geochemical modeling package: revised algorithm and GEMS3K numerical kernel for coupled simulation codes, Comput. Geosci. 17 (2013) 1–24. https://doi.org/10.1007/s10596-012-9310-6.

[9] T. Wagner, D.A. Kulik, F.F. Hingerl, S. V Dmytrieva, GEM-Selektor geochemical modeling package: TSolMod library and data interface for multicomponent phase models, Can. Mineral. 50 (2012) 1173–1195. https://doi.org/10.3749/canmin.50.5.1173.

[10] T. Thoenen, W. Hummel, U. Berner, E. Curti, The PSI/Nagra Chemical Thermodynamic Database 12/07, PSI report 14-04, Villigen PSI, Switzerland, (2014).

[11] B. Lothenbach, D.A. Kulik, T. Matschei, M. Balonis, L. Baquerizo, B. Dilnesa, G.D. Miron, R.J. Myers, Cemdata18: A chemical thermodynamic database for hydrated Portland cements and alkali-activated materials, Cem. Concr. Res. 115 (2019) 472–506. https://doi.org/10.1016/j.cemconres.2018.04.018.

[12] R.J. Myers, S.A. Bernal, J.L. Provis, A thermodynamic model for C-(N-) ASH gel: CNASH_ss. Derivation and validation, Cem. Concr. Res. 66 (2014) 27–47. https://doi.org/10.1016/j.cemconres.2014.07.005.

[13] Z. Shi, B. Lothenbach, The role of calcium on the formation of alkali-silica reaction products, Cem. Concr. Res. 126 (2019) 105898. https://doi.org/10.1016/j.cemconres.2019.105898.

[14] Z. Shi, A. Leemann, D. Rentsch, B. Lothenbach, Synthesis of alkali-silica reaction product structurally identical to that formed in field concrete, Mater. Design 190 (2020) 108562.

[15] Z. Shi, B. Lothenbach, The combined effect of potassium, sodium and calcium on the formation of alkali-silica reaction products, Cem. Concr. Res. 127 (2020) 105914. https://doi.org/10.1016/j.cemconres.2019.105914.

[16] G.M. Anderson, D.A. Crerar, Thermodynamics in Geochemistry: The Equilibrium Model, Oxford University Press, Oxford, 1993.

[17] B. Lothenbach, T. Matschei, G. Möschner and F.P. Glasser, Thermodynamic modelling of the effect of temperature on the hydration and porosity of Portland cement. Cem. Concr. Res. 38) (2008) 1-18.

[18] J. Lindgård, Ö. Andiç-Çakır, I. Fernandes, T.F. Rønning, M.D.A. Thomas, Alkali–silica reactions (ASR): literature review on parameters influencing laboratory performance testing, Cem. Concr. Res. 42 (2012) 223–243.

[19] Z. Shi, C. Shi, S. Wan, Z. Zhang, Effects of alkali dosage and silicate modulus on alkali-silica reaction in alkali-activated slag mortars, Cem. Concr. Res. 111 (2018) 104–115. doi:10.1016/j.cemconres.2018.06.005.